Molecular Biology of the Cell
Vol. 7, 2029–2044, December 1996

# Role of 26S Proteasome and *HRD* Genes in the Degradation of 3-Hydroxy-3-Methylglutaryl-CoA Reductase, an Integral Endoplasmic Reticulum Membrane Protein

**Randolph Y. Hampton,*† Richard G. Gardner,* and Jasper Rine‡**

*Department of Biology, University of California, San Diego, La Jolla, California 92093-0116; and
‡Molecular Cell Biology Department, Division of Genetics, University of California, Berkeley, Berkeley, California 94720

Submitted August 6, 1996; Accepted September 18, 1996
Monitoring Editor: Michael H. Wigler

3-hydroxy-3-methylglutaryl-CoA reductase (HMG-R), a key enzyme of sterol synthesis, is an integral membrane protein of the endoplasmic reticulum (ER). In both humans and yeast, HMG-R is degraded at or in the ER. The degradation of HMG-R is regulated as part of feedback control of the mevalonate pathway. Neither the mechanism of degradation nor the nature of the signals that couple the degradation of HMG-R to the mevalonate pathway is known. We have launched a genetic analysis of the degradation of HMG-R in *Saccharomyces cerevisiae* using a selection for mutants that are deficient in the degradation of Hmg2p, an HMG-R isozyme. The underlying genes are called *HRD* (pronounced "herd"), for HMG-CoA reductase degradation. So far we have discovered mutants in three genes: *HRD1*, *HRD2*, and *HRD3*. The sequence of the *HRD2* gene is homologous to the p97 activator of the 26S proteasome. This p97 protein, also called TRAP-2, has been proposed to be a component of the mature 26S proteasome. The *hrd2-1* mutant had numerous pleiotropic phenotypes expected for cells with a compromised proteasome, and these phenotypes were complemented by the human TRAP-2/p97 coding region. In contrast, *HRD1* and *HRD3* genes encoded previously unknown proteins predicted to be membrane bound. The Hrd3p protein was homologous to the *Caenorhabditis elegans* sel-1 protein, a negative regulator of at least two different membrane proteins, and contained an HRD3 motif shared with several other proteins. Hrd1p had no full-length homologues, but contained an H2 ring finger motif. These data suggested a model of ER protein degradation in which the Hrd1p and Hrd3p proteins conspire to deliver HMG-R to the 26S proteasome. Moreover, our results lend in vivo support to the proposed role of the p97/TRAP-2/Hrd2p protein as a functionally important component of the 26S proteasome. Because the *HRD* genes were required for the degradation of both regulated and unregulated substrates of ER degradation, the *HRD* genes are the agents of HMG-R degradation but not the regulators of that degradation.

## INTRODUCTION

Protein degradation is an essential function that has many roles in all eukaryotic cells (Bienkowski, 1983; Hochstrasser, 1992; Bour *et al.*, 1995; Grant *et al.*, 1995). Mutant, modified, or misassembled proteins all require disposal (Schuller *et al.*, 1992; Tierney *et al.*, 1992; Tsuji *et al.*, 1992; Pearce and Sherman, 1995). Viral invasion strategies can include degradative tactics (Scheffner *et al.*, 1993; Bour *et al.*, 1995; Wiertz *et al.*,

† Corresponding author.

1996). Signaling cascades can be started or halted by selective degradation (Jabben *et al.*, 1989; Glotzer *et al.*, 1991; Papavassiliou *et al.*, 1992). Finally, the steady-state levels of many key proteins are regulated by altering their degradation rates (Murakami *et al.*, 1992; Hampton and Rine, 1994; Kornitzer *et al.*, 1994). Protein degradation represents a chapter of cellular regulation that is just beginning to be written. In all examples of selective protein degradation, the principle questions are: 1) how are specific proteins targeted for degradation; and 2) what is the mechanism of their degradation.

For soluble proteins, two main themes have emerged as determinants of protein stability. One theme is that some proteins are relocated to the lysosome, or the vacuole in yeast, where they are degraded. Soluble proteins in membrane-bound compartments are moved to these degradative organelles by vesicular traffic. However, this mechanism also operates on cystolic proteins, indicating the existence of a mechanism for translocation of these proteins across the membrane of the lysozyme or vacuole (Dice and Chiang, 1989; Chiang and Schekman, 1991; Scott and Klionsky, 1995; Oda *et al.*, 1996). A second theme, operating on other soluble proteins, involves targeting the proteins for degradation by the 26S proteasome, often (but not always) by addition of ubiquitin (Finley and Chau, 1991; Hochstrasser, 1995). Some proteins are degraded either in the cytoplasm by the proteasome or by translocation into the vacuole, depending on experimental circumstances (Chiang and Schekman, 1991; Schork *et al.*, 1995). Both routes to degradation use specific amino acid sequences of the protein to direct its selection for destruction.

The degradation of membrane proteins, although less well understood, also appears to involve at least two distinct routes. Some membrane proteins are trafficked to the lysosome or vacuole by vesicular transport (Wilcox *et al.*, 1992; Berkower *et al.*, 1994). In contrast, the destruction of certain endoplasmic reticulum (ER) proteins, such as the CFTR protein, the unassembled T-cell receptor subunits, and 3-hydroxy-3-methylglutaryl-CoA (HMG-R), appears to occur in situ in the ER without the need for traffic to a degradative compartment.

The molecular mechanisms of selective membrane protein degradation, including ER proteins, is an active frontier in cell biology. Use of novel protease inhibitors has suggested that the 26S proteasome may play a role in the ER degradation of the CFTR protein (Jensen *et al.*, 1995; Ward *et al.*, 1995). However data derived from proteasomal inhibitors, as with most inhibitors, can be difficult to interpret (Jensen *et al.*, 1995). If the proteasome is involved in the degradation of membrane proteins, it is unclear how a membrane protein would be specifically targeted for degradation by a soluble complex such as the proteasome. It is similarly unclear how degradation of proteins that span organellar membranes can be processive. The complete removal of the degradation substrate from the membrane (Wiertz *et al.*, 1996) or sequential cleavage by different proteases in distinct compartments have each received experimental support as possible strategies around the topological barriers to processive degradation (Mullins *et al.*, 1995).

To identify the molecules that mediate selective degradation of ER membrane proteins, we have launched a genetic analysis of the degradation of HMG-R. HMG-R is of particular interest as a degradation substrate for several reasons. Because this integral membrane protein is a substrate for degradation in both yeast and mammals, it is a reasonable guide to the underlying general features that determine eukaryotic membrane protein stability. In both yeast and humans, the ER degradation of HMG-R is subject to feedback regulation by the mevalonate pathway as part of the regulation of sterol synthesis: high flux through the mevalonate pathway results in a high degradation rate of HMG-R, whereas slowed flux through the mevalonate pathway results in slowed degradation of HMG-R (Edwards *et al.*, 1983; Goldstein and Brown, 1990; Roitelman and Simoni, 1992; Hampton and Rine, 1994). The molecular mechanisms of regulated HMG-R degradation should reveal how cells control the stability of membrane proteins. These studies should also identify the specific molecules that cells use to monitor the mevalonate pathway and reveal how the level of these molecules is coupled to HMG-R degradation.

We have previously shown that degradation of the HMG-R isozyme Hmg2p of *Saccharomyces cerevisisae* is regulated by the mevalonate pathway in a manner similar to that observed for mammalian HMG-R (Hampton and Rine, 1994; Hampton *et al.*, 1996). By designing a selection for mutants deficient in the degradation of yeast Hmg2p, we have defined and isolated genes responsible for the degradation of the Hmg2p isozyme and related substrates. These genes are called *HRD* genes (pronounced "herd"), for **H**MG-CoA **R**eductase **D**egradation. The identities of these genes suggested a mechanism for degradation of Hmg2p that involves recognition of this protein in the membrane followed by degradation of the protein by the 26S proteasome. Our results indicated that the 26S proteasome was broadly involved in the degradation of membrane proteins, and that novel molecules may bring about earlier steps in the degradation process that allow recognition by this general proteolytic complex.

## MATERIALS AND METHODS

### *Materials*

The anti-myc 9E10 antibody was used either as ascites fluids (provided by R. Schekman, University of California, Berkeley, Berkeley, CA) or as cell culture supernatant obtained by growing the 9E10 hybridoma (ATCC CRL 1729) in RPMI 1640 culture medium (Life Technologies, Grand Island NY) with 10% fetal calf serum. Affinity-purified polyclonal antiubiquitin antibody was generously provided by Arthur Haas (Wisconsin Medical College, Milwaukee, WI; Tierney *et al.*, 1992). All other reagents were obtained as described previously (Hampton and Rine, 1994; Hampton *et al.*, 1996).

### *Yeast Culture and Strains*

Yeast were grown and transformed using the media, conditions, and techniques described earlier (Hampton and Rine, 1994; Hampton *et al.*, 1996). All experiments were conducted in yeast minimal medium (0.67% yeast nitrogen base; Difco, Detroit, MI) supplemented as needed. RHY244, the parent strain for the HRD selection, was prepared by transforming the mevalonate auxotrophic strain RHY468 (alias JRY1593; *a, ade2-101, his3Δ200, lys2-801, ura3-52, met, hmg1::LYS2, hmg2::HIS3*) with plasmid pRH244 that expresses the *6MYC-HMG2* coding region (see below) at the *Stu*I site in the *ura3-52* locus. RHY244 was thus a $Ura^+$,$Mev^+$ strain that produced only the 6myc-Hmg2p variant, whose half-life was unregulated, from a single copy of the coding region expressed from the strong, constitutive glyceraldehyde-3-phosphate dehydrogenase (GAPDH) promoter (previously called the GPD promoter; Hampton and Rine, 1994; Hampton *et al.*, 1996). Strain RHY183 expressed normal Hmg2p from the same GAPDH promoter (Hampton and Rine, 1994). Candidate mutants from the HRD selection were cured of the original integrated pRH244, and thus restored to $Ura^-$,$Mev^-$ status, by growth of each strain on 5-fluoro orotic acid (5-FOA) plates supplemented with 10 mg/ml mevalonic acid (Boeke *et al.*, 1987). These strains were used to test each mutant for plasmid independence of the mutant phenotypes under study by retransformation with pRH244, to restore the expression of 6myc-Hmg2p, and testing for phenotypes. The same $Ura^-$,$Mev^-$ strains were also transformed with plasmids expressing normal Hmg2p from the GAPDH promoter to examine the effects of each mutation on the degradation of normal Hmg2p. $Ura^-$ versions of each mutant strain and the original parent were also prepared from the resulting $Ura^-$ $Mev^-$ auxotrophs by integrative transformation with pRH405, a variant of pRH244 that had an *Aat*II/*Ppu*MI fragment containing the entire promoter and 5′ coding region of *URA3* removed. The resulting plasmid could still be integrated at the *ura3-52* locus site and resulted in a strain that expressed the 6myc-Hmg2p ($Mev^+$) but remained $Ura^-$. Such $Mev^+$ $Ura^-$ strains were prepared from the wild-type parent and the three mutants *hrd1-1*, *hrd2-1*, and *hrd3-1* and were named RHY400, 401, 402, and 403, respectively. The resulting three mutant strains were used as recipients of a YCp50-based genomic library (*URA3* marker) to clone the wild-type *HRD* genes (Rose *et al.*, 1987). Strains RHY513 and RHY514, which expressed the normally regulated Hmg2p-GFP fluorescent reporter protein (Hampton *et al.*, 1996), were made by transforming RHY400 ($Hrd^+$) and RHY401(*hrd1-1*) with pRH469, an integrating plasmid containing the *HMG2::GFP* coding region (with the S65T bright mutation in the GFP coding region) under the control of the GAPDH promoter to examine the dynamics of the Hmg2p-GFP reporter protein in a *hrd1-1* mutant. pRH469 was integrated at the *ura3-52* locus, and transformants were selected for $Ura^+$.

### *Molecular Cloning*

The 6myc-Hmg2p protein was expressed from plasmid pRH244. pRH244 was made by altering the *HMG2* coding region in the integrating *URA3* plasmid pRH144-2 that expressed the *HMG2* coding region from the GAPDH promoter (Hampton and Rine, 1994). The term GPD has been used on numerous occasions by us and others (e.g., Schena *et al.*, 1991) to indicate the GAPDH promoter as cloned and characterized by Bitter and Egan (1984). However, there are two other yeast genes designated *GPD1* and *GPD2* that do not encode GAPDH, but rather *sn*-glycerol-3-phosphate dehydrogenase ($NAD^+$), which are highly regulated enzymes subject to numerous controls (Eriksson *et al.*, 1995). Therefore, we now refer to the strong constitutive promoters used herein and in our previous studies as pGAPDH to distinguish them from the unrelated *GPD* genes.

The *6MYC-HMG2* coding region was prepared by inserting a 299-bp *Hin*cII/*Spe*I fragment containing six tandem myc epitopes from pRH360 into the *Aat*II (blunt) and *Spe*I sites of pRH144-2 (Hampton and Rine, 1994). The result of this cloning was to replace most of the first putative cytosolic loop of Hmg2p with a similarly sized in-frame fragment encoding six tandem myc epitope tags (Evan *et al.*, 1985; Figure 1A). The YCp50-based (ARS/CEN, *URA3*) yeast genomic library used to clone the three *HRD* genes was provided by Paul Herman (University of California, Berkeley). Plasmid pRH469, which expressed the *HMG2::GFP(S65T)* "bright" version of the previously described *HMG2::GFP* coding region (Hampton and Rine, 1994), was prepared by replacing the *Msc*I/*Sal*I of pRH408 with the corresponding *Msc*I/*Sal*I fragment of pS65T-C1 (CLONETECH, Palo Alto, CA) to introduce the S65T mutation into the GFP portion of the HMG2-GFP coding region. The TRAP-2 coding region was cloned from the plasmid pTRAP-SK, with the TRAP-2 coding region cloned into Bluescript II SK, provided by Dr. David Donner (University of Indiana Medical Center, Indianapolis, IN), into the integrating *URA3* plasmid pRH98-1 (ARS/CEN, *URA3*) so that the coding region was under the control of the GAPDH promoter. pRH98-1 was made in the same manner as pRH98-2 (Hampton and Rine, 1994), but with the ARS/CEN parent vector Yplac33 instead of the integrating Yplac211 (Gietz and Sugino, 1988). We noted that a portion of the TRAP-2 cDNA, originally designated as a portion of untranslated leader upstream of the ATG codon, in fact encoded ~37 more amino acids that were nearly identical to the corresponding amino acids in the longer submission in the database (see below) called human 26S proteasomal subunit p97. The 37 extra amino acids encoded in the leader region are SGGTDEKPSGKGRRDAGDKDKELELSEEDKQLQDELV. Accordingly, we designed a synthetic linker that provided a new ATG in-frame to this upstream portion to produce a protein in yeast that included these extra amino acids. The linker was produced by annealing the two oligonucleotides: 5′-GATCCCCATGGCCT-GCA-3′ and 5′-GGCCATGGG-3′. When used as described, the linker added the peptide MACRN to the 37-amino acid extension to TRAP-2 listed above, thus providing a new upstream start codon. The distal *Pst*I site 3′ to the stop codon of TRAP-2 was removed. The ATG-providing linker was next cloned into the remaining *Pst*I and *Bam*HI sites immediately 5′ to the start of the coding region. Finally the *Bam*HI/*Sal*I fragment with the now extended coding region was placed in the same sites of pRH98-2 to yield pRH497.

### *HRD Selection*

The wild-type ($Hrd^+$) parent strain was RHY244 (*hmg1::LYS2, hmg2::HIS3, ura3-52::pGAPDH-6MYC-HMG2::URA3*), which expressed only the 6myc-Hmg2p, whose half-life was unregulated, as its sole source of essential HMG-R activity. Selection plates consisted of minimal solid medium (0.67% Difco yeast nitrogen base/2% glucose) supplemented with adenine sulfate (30 mg/l) and methionine (30 mg/l) and containing 200 μg/ml of lovastatin, a competitive inhibitor of HMG-R. Cells from individual clonal liquid cultures of nonmutagenized RHY244 were plated onto solid supplemented minimal medium containing lovastatin at a density of ~$2 \times 10^6$ cells/plate and incubated at 34°C until discrete colonies appeared in 1–2 wk. Typically, a plate had between 1 and 10 colonies. A total of 20 plates was used for the HRD selection. Individual colonies from the plates were grown on supplemented

minimal medium plates without lovastatin and then tested for maintained resistance following nonselective growth. True-breeding candidates were evaluated for steady-state levels of the 6myc-Hmg2p protein by immunoblotting lysates from log-phase cultures for myc immunoreactivity. Finally, strains were tested for stabilization of the 6myc-Hmg2p by immunoblotting after growth into the stationary phase (see below). Promising candidates were chosen such that each candidate came from a different selection plate and were thus independent. Final candidates were then tested by cycloheximide-chase and pulse-chase to determine whether the effects on the steady-state level of 6myc-Hmg2p were attributable to alterations in the degradation. Each candidate with stabilized 6myc-Hmg2p was cured of the original 6myc-Hmg2p expression plasmid (to give Mev$^-$ Ura$^-$ cells) and then was retransformed with pRH244 to test for plasmid independence of the phenotypes. The same Mev$^-$ Ura$^-$ cells were also transformed with a plasmid expressing normal Hmg2p from the GAPDH promoter to test the ability of each candidate to degrade the normal Hmg2p protein.

## Genetic Analysis of the hrd Mutants

The mutations that stabilized 6myc-Hmg2p were tested for dominance by mating each to an $\alpha$ version of the parent strain, by isolating zygotes from a mating mixture, to form diploids that were isogenic (except for any mutations) to the original strain. The resulting diploids were then tested for lovastatin resistance and stabilization of the 6myc-Hmg2p protein. The diploids were sporulated and the resulting haploid progeny analyzed for lovastatin resistance and stabilization of the 6myc-Hmg2p protein. The distribution of the Hrd$^-$ phenotype among the progeny was used to evaluate the number of loci underlying the phenotype of each mutant.

To perform complementation analysis of the mutants, a representative $\alpha$ mating-type strain was recovered for each mutant from the tetrad analysis. Mutant strains of both mating types were used to make diploids heterozygous for different mutations. Each diploid was tested for stabilization of 6myc-Hmg2p. Each heterozygous diploid was then sporulated and separated into haploid progeny. The pattern and frequency of lovastatin resistance among the progeny indicated whether the two combined mutations in a given heterozygote were allelic or unlinked. These analyses revealed the existence of three unlinked loci, *HRD1*, *HRD2*, and *HRD3*, in which recessive mutations stabilized both 6myc-Hmg2p and Hmg2p.

## Cloning of the HRD Genes

Representative *hrd* mutants were chosen for cloning the wild-type allele by plasmid complementation. These mutants are referred to as *hrd1-1*, *hrd2-1*, and *hrd3-1*. For each of these mutants, the Mev$^-$ Ura$^-$ strain that was made by 5-FOA-selected loss of the 6myc-Hmg2/URA3 plasmid was transformed with a variant of the pRH405 plasmid (6myc-Hmg2p, *ura3*$\Delta$, see above), allowing restored expression of the 6myc-Hmg2p, in cells that were Ura$^-$. The resulting Hrd$^-$, Mev$^+$, Ura$^-$ strains, each bearing a single recessive *hrd* mutation, were called RHY401, 402, and 403 and harbored the *hrd1-1*, *hrd2-1*, and *hrd3-1* mutations, respectively. Each mutant was transformed with a yeast genomic library (YCp50 (ARS/CEN); Rose *et al.*, 1987) selecting for Ura$^+$ transformants. Master plates of the resulting Ura$^+$ colonies were replica plated onto supplemented minimal medium with lovastatin to identify colonies that regained wild-type sensitivity to lovastatin. Plasmids were recovered from candidate lovastatin-sensitive colonies and retested by retransformation of the mutant strain. Purified plasmids that could restore wild-type lovastatin sensitivity and 6myc-Hmg2p degradation to a given *hrd* mutation were analyzed by sequencing the flanks of the particular ends of the insert DNA using sequencing primers flanking the YCp50 *Bam*HI site. This information was used to ascertain the genomic location of the insert. Each plasmid was then analyzed by subcloning to test each candidate coding region in a given insert for the ability to complement the appropriate *hrd* mutant. Finally, each single candidate coding region was cloned into an integrating (YIp, *URA3*) plasmid, integrated at its homologous genomic location in an $\alpha$, *ura3* version of the Hrd$^+$ parent strain (RHY454). The resulting strain with the cloned locus marked with the *URA3* gene was crossed to the corresponding Ura$^-$ *hrd* mutant. The resulting diploid with the cloned gene marked with *URA3* was then subjected to tetrad analysis and examined for segregation of the *URA3* marker and the *hrd* mutation. The segregation of 2 Hrd$^+$:2 Hrd$^-$ and 2 Ura$^+$:2 Ura$^-$ in all tetrads such that the Ura$^+$ cells were always Hrd$^+$ (and the Ura$^-$ cells were always Hrd) was genetic proof of having cloned the wild-type gene underlying the *hrd* mutation under study.

## Access to Sequence Information

Each of the protein (and corresponding nucleotide) sequences mentioned in this work are in public databases as follows. Unless otherwise noted, the numbers are for GenBank entries: Hrd2p: U10399, coding region YHR027c; TRAP-2: U12596; human 26S proteasome subunit p97: *D78151*; Sen3p: L06321; Hrd3p: PIR database S48558; hypothetical protein L8167.5; sel-1: U50828 and U50829; Ibd2: U11037; *Schizosaccharomyces pombe* unknown protein: D83992, coding sequence 3030–3566; and Skt5p: S65415. The *HRD1* gene can be accessed on the World Wide Web (http://genome-www.stanford.edu/*Saccharomyces*/); Hrd1p: PID g1419785; coding region YOL013c.

## Analysis of Protein Stability

The stability of 6myc-Hmg2p and Hmg2p were assayed in three ways, each of which has been described (Hampton and Rine, 1994; Hampton *et al.*, 1996). Briefly, they are as follows: 1) pulse-chase analysis using $^{35}$S labeling followed by immunoprecipitation; 2) cycloheximide chase in which log phase cells are treated with cycloheximide and periodically immunoblotted to follow the degradation of the entire pool of a particular protein; and 3) "stationary chase" in which cells are grown ~12-15 h at 30°C after the cells have attained a mid-log phase (~0.5 $OD_{600}$) culture density to achieve the stationary phase followed by immunoblotting. The "stationary chase" reports the continued degradation of the pool of protein under study after protein synthesis has ceased due to the depletion of nutrients. This method reports the regulated degradation of Hmg2p and that of Hmg2p-GFP (Hampton *et al.*, 1996). Preparations of cell lysates for immunoblotting were made as described (Hampton and Rine, 1994). The myc tag was sufficiently specific in these strains to allow dot blotting of the crude lysates for the specific detection of the 6myc protein. Lysates were placed in a 96-well dish and transferred by a multiprong transfer device (Sigma, St. Louis, MO) to a piece of dry nitrocellulose, which was then processed for immunoblotting. Immunoblotting for the myc tag, whether by dot-blotting or gel-immunoblotting, was performed as described for anti-Hmg2p (Hampton and Rine, 1994), except that the 9E10 monoclonal anti-myc antibody was used at a 1:2000 dilution of murine ascites fluid or a 1:5 dilution of hybridoma supernatant, and the secondary antibody was goat anti-mouse horseradish peroxidase (HRP) (Life Technologies, Grand Island, NY). The ECL detection reagents (Amersham, Arlington Heights, IL) were used in all immunoblotting procedures.

## GFP Fluorescent Microscopy

The fluorescence of strains expressing the *HMG2::GFP(S65T)* gene in a wild-type (RHY513) or *hrd1-1* (RHY514) background was evaluated by fluorescence microscopy using a Nikon Optiphot II microscope with a Cohu (San Diego, CA) CCD, a Colorado Video Integrator (Boulder, CO), and a Sony graphic printer. The images shown were directly digitized on a Hewlett-Packard Scanjet 3C scanner.

The cells were grown into stationary phase from cultures of $OD_{600}$ 0.5 for 15 h and photographed directly from the cultures.

### *Global Ubiquitination Assay*

Ubiquitination of total cellular proteins was assessed by immunoblotting whole-cell lysates with an affinity-purified polyclonal rabbit anti-ubiquitin antibody.

## RESULTS

To study the regulated degradation of yeast Hmg2p in isolation from any other possible form of regulation, we used strains that express Hmg2p, but not the Hmg1p isozyme, from a single integrated copy of the *HMG2* gene whose promoter has been replaced by the more powerful constitutive GAPDH promoter. As previously demonstrated (Hampton and Rine, 1994; Hampton *et al.*, 1996), Hmg2p expressed in this manner is subject to regulated degradation. Thus, strains constitutively expressing Hmg2p in this way have a steady-state level of HMG-R activity that is determined entirely by the high constitutive synthesis rate combined with the rate of degradation.

The selection for mutants deficient in Hmg2p degradation was based on the prediction that such mutants would have a higher steady-state level of Hmg2p. Because the HMG-R enzyme activity is essential, drugs that inhibit HMG-R, such as lovastatin, kill cells in a dose-dependent manner. Thus, mutants with a higher steady-state level of HMG-R would be expected to have heightened resistance to lovastatin and therefore be selectable from wild-type cells in growth medium containing a normally toxic dose of the drug.

The selection for degradation mutants was first attempted with a strain that lacked both endogenous HMG-R genes (*hmg1::LYS2* and *hmg2:HIS3*) and had a single integrated copy of the *HMG2* gene driven by the constitutive GAPDH promoter. Growth of this strain was blocked by lovastatin in a dose-dependent manner (Figure 1D, ovals). However, even at the highest practical doses of the drug, the plating efficiency of surviving colonies was on the order of 0.1–1% for nonmutagenized cells. Furthermore, the survivors did not remain lovastatin resistant after outgrowth in the absence of the drug. Thus, the lovastatin resistance that the surviving colonies acquired was the result of physiological, rather than genetic, changes in the cells. We reasoned that the high-plating efficiency on medium containing lovastatin might be due, at least in part, to the cell's ability to slow Hmg2p degradation, increasing Hmg2p steady-state level, when lovastatin slowed the mevalonate pathway. In effect, lovastatin would induce higher levels of its own target. In this way the normal regulation of Hmg2p stability would blunt the effects of lovastatin and hinder the recovery of mutants.

### *6myc-Hmg2p: an Unregulated Reductase*

To remove the contribution of regulated degradation to the high survival rate in the selection, we developed a variant of the Hmg2p molecule, 6myc-Hmg2p (Figure 1A), whose degradation was not regulated by alterations in the mevalonate pathway (Figure 1, B and C). The addition of a small dose of lovastatin to cultures dramatically stabilized wild-type Hmg2p, whereas the degradation of the 6myc-Hmg2p molecule was unaffected. Two independent assays of whole-pool degradation were used: addition of cycloheximide to the cells followed by immunoblotting (Figure 1B), and growth of the cells into early stationary phase such that the synthesis of protein ceases while degradation proceeds, also followed by immunoblotting (Figure 1C). In both procedures the degradation of Hmg2p was strongly inhibited by slowing the mevalonate pathway, whereas the degradation of the 6myc-Hmg2p protein was unaffected. Thus, conditions known to stabilize Hmg2p had no effect on 6myc-Hmg2p. In all other ways, the 6myc-Hmg2p protein behaved like Hmg2p. 6myc-Hmg2p complemented lethal mutations in the wild-type *HMG-R* genes. Like Hmg2p, 6myc-Hmg2p protein was an integral membrane protein that could be solubilized only by detergent treatment (our unpublished observation). Finally, 6myc-Hmg2p was degraded at a similar rate to Hmg2p under normal growth conditions (0.5–1-h half-life), and degradation was independent of vacuolar proteases or the secretory pathway (our unpublished observation). Curiously, the electrophoretic mobility of the 6myc-Hmg2p protein was less than would be predicted from the sequence of the coding region. Although the protein would be expected to be nearly identical in mass to normal Hmg2p (~115 kDa), the mobility of 6myc-Hmg2p reproducibly ran at a position on denaturing SDS-polyacrylamide gels that was expected for a protein of ~140 kDa. This difference in mobility is shown in Figure 1C, in which the two panels are aligned as on the original gel. The altered mobility of the 6myc variant was not due to *N*-linked glycosylation (our unpublished observation).

A comparison of otherwise isogenic strains expressing either the *HMG2* gene or the *6MYC-HMG2* gene from the strong GAPDH promoter at the same integration site revealed that the strain expressing the 6myc-Hmg2p unregulated construct was more sensitive to lovastatin in liquid medium (Figure 1D, diamonds). When cells that expressed 6myc-Hmg2p (RHY244) were plated on solid lovastatin-containing medium, the plating efficiency was on the order of 1 in $10^6$ as compared with the ~1% observed with the isogenic strain (RHY183) that expressed wild-type Hmg2p. It would appear that the loss of regulation of 6myc-Hmg2p degradation indeed resulted in a greater

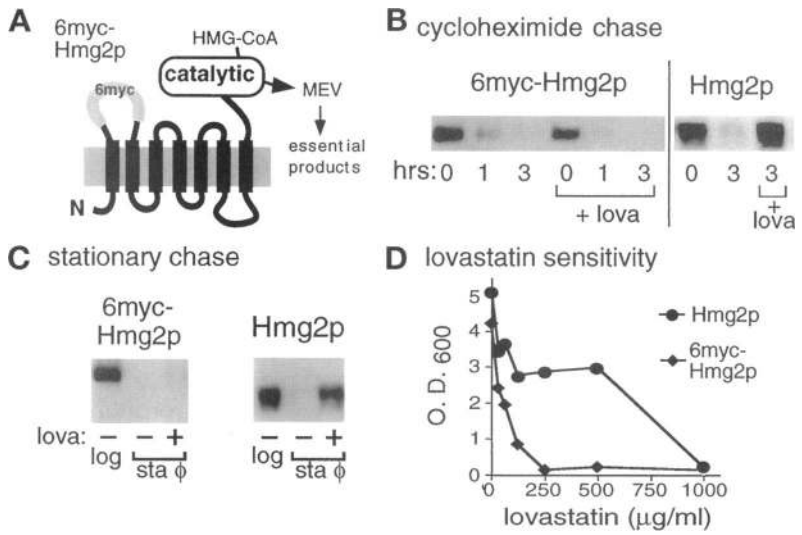


**Figure 1.** 6myc-Hmg2p: an unregulated variant of Hmg2p. (A) Schematic diagram of the unregulated 6myc-Hmg2p. The 6myc protein had a portion of the protein sequence replaced between the first two putative transmembrane spans (see Basson *et al.*, 1988) with six tandem myc epitope tags. The tagged protein was still capable of catalyzing the reduction of HMG-CoA to mevalonate (MEV), an essential intermediate of cholesterol biosynthesis. (B) The degradation of 6myc-Hmg2p was not regulated by the mevalonate pathway. Cells expressing 6myc-Hmg2p (RHY244) or Hmg2p (RHY183) were examined for degradation of each protein by addition of cycloheximide at time 0 and subsequent immunoblotting as described (Hampton and Rine, 1994). In the indicated samples, 50 μg/ml of lovastatin were added along with the cycloheximide at $t = 0$. The 6myc-Hmg2p lanes (left panel) were immunoblotted using the 9E10 anti-myc antibody, and the Hmg2p lanes (right panel) were immunoblotted with affinity-purified anti-Hmg1p protein. Each lane contained lysate from ~0.2 $OD_{600}$ U of cells. (C) Test of 6myc-Hmg2p degradation by stationary chase. Log phase (~0.5 $OD_{600}$) cultures of the strains used in B were allowed to grow for an additional 15 h at 30°C and then subjected to lysis and immunoblotting to evaluate degradation of the expressed reductase (Hampton *et al.*, 1996). In the samples labeled "+", 50 μg/ml lovastatin were added to the cultures at the mid-log phase, and the cultures were then incubated an additional 15 h. The lanes labeled "log" were prepared from cultures that were diluted at the start of the 15-h incubation period such that they were in log phase at the time all samples were harvested. All samples were immunoblotted with the anti-HmgRp antiserum used in the Hmg2p samples in B. Note the lowered mobility of the 6myc-Hmg2p protein as compared with the native Hmg2p. The lanes from the 6myc-Hmg2p-expressing strain were loaded with three times as much total protein to allow direct comparison of the two signals. (D) Lovastatin sensitivity of strains expressing either 6myc-Hmg2p (RHY244) or Hmg2p (RHY183), as marked. Cultures of cells at a low starting $OD_{600}$ (~0.05) were grown in the presence of increasing amounts of lovastatin for 5 days. Final ODs of cultures at each dose are shown.

sensitivity to lovastatin. It should be noted that the steady-state level of the 6myc-Hmg2p, as measured by immunoblotting, was approximately threefold less than the steady-state level of wild-type Hmg2p expressed in the same strains under the same conditions. The reason for this quantitative difference was unknown. Nevertheless, the drastically decreased plating efficiency of strains with 6myc-Hmg2p on lovastatin allowed the successful selection of the *hrd* mutants described below.

### *HRD Selection*

Mutants defective in the degradation of HMG-R would identify the underlying machinery that brings about the degradation of this enzyme. The mutants defined the *HRD* genes (pronounced "herd"). The selection that resulted in isolation of these mutants, known as the HRD selection, is represented in Figure 2. In a strain expressing only the 6myc-Hmg2p protein, which had an unregulated half-life, lovastatin sensitivity was a simple indicator of Hmg2p steady-state levels, because the drug itself no longer slowed the degradation of Hmg2p. Cells with an elevated steady-state level of 6myc-Hmg2p caused by a *hrd* mutation (right panel, ×) were selected by plating cells expressing the 6myc-Hmg2p as their only form of HMG-R on medium containing lovastatin (~1 in $10^6$ plating efficiency). The plates were incubated at 34°C and allowed to grow for ~1 wk. The elevated temperature was chosen because the selection works quickly at this temperature.

Resistant colonies were tested for three different phenotypes as described in MATERIALS AND METHODS: 1) continued lovastatin resistance follow-

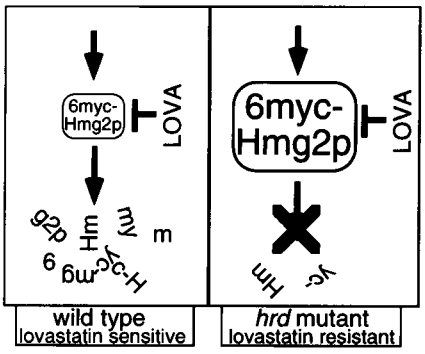


**Figure 2.** The HRD selection. The steady-state level of HMG-R activity and the corresponding sensitivity to lovastatin are determined by the balance between the synthesis (top arrow) and degradation (bottom arrow) of the 6myc-Hmg2p protein. A strain (RHY244) expressing only the unregulated 6myc-Hmg2p from the GAPDH promoter from a gene integrated into genome was lovastatin sensitive. A mutation that slows degradation (×) caused an increase in the steady-state level of the 6myc-Hmg2p protein and a corresponding increase in lovastatin resistance.

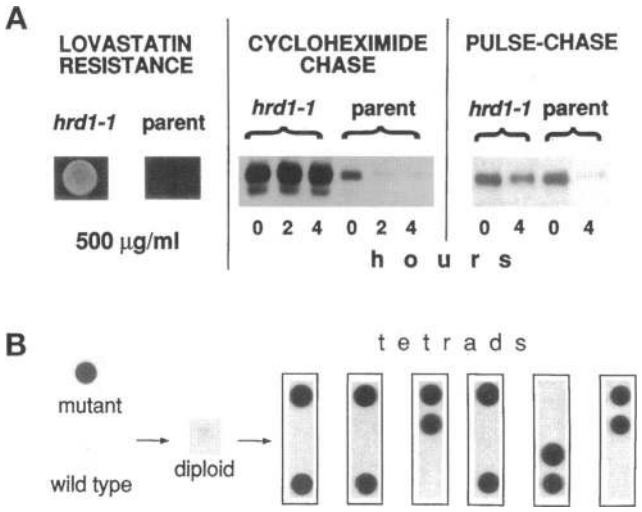


**Figure 3.** The *hrd1-1* mutant and the Hrd$^-$ phenotype. (A) A profile of the phenotypes of a representative *hrd* mutant, *hrd1-1*, relative to wild type. Lovastatin resistance (left) was tested by spotting 20 μl of an OD 0.1 culture onto supplemented minimal medium with the indicated concentrations of lovastatin and allowing growth for 1 wk. Note that the *hrd1-1* strain was resistant to a dose of lovastatin higher than the concentration used in the selection. The degradation of the entire pool of 6myc-Hmg2p (middle panel, cycloheximide chase) was determined by addition of cycloheximide to log phase cultures of mutant or wild-type cells at $t = 0$ and subsequently immunoblotting of the lysate with the 9E10 anti-myc antibody. Each lane received lysate from 0.2 OD U of cells. The $t = 0$ lanes indicated that there was increased steady-state 6myc-Hmg2p protein in the mutant. Pulse-chase experiments were performed on each strain but with the anti-myc 9E10 antibody (10 μl of ascites) as the precipitating antibody (right panel). The $t = 0$ lane revealed that the synthetic rate of the 6myc-Hmg2p protein in each strain was comparable. (B) Mendelian genetics of the mutant. Lysates from the *hrd1-1* strain, the wild-type parent strain of opposite mating type, the diploid from these two, and the haploid progeny of six representative tetrads were analyzed for myc immunoreactivity after growth into stationary phase. Because of the specificity of the myc tag, the lysates were analyzed by dot immunoblotting. A dark signal indicates slow degradation due to the *hrd* mutation. The mutation was recessive because the diploid had normal degradation of 6myc-Hmg2p and the phenotype segregated as a single locus, since degradation:stabilization segregated 2:2.

ing nonselective growth; 2) increased steady-state levels of 6myc-Hmg2p; and 3) increased half-life of 6myc-Hmg2p, as shown for the *hrd1-1* mutant (Figure 3A). The *hrd1-1* mutant clearly was more resistant to lovastatin than the wild-type parent (Figure 3A, left panel). The concentration of lovastatin used in this experiment was significantly higher than that used in the selection itself (500 vs. 200 μg/ml). To assess the stability of the entire 6myc-Hmg2p pool, log phase cultures were treated with cycloheximide at time 0 and subjected to immunoblotting analysis with the 9E10 anti-myc monoclonal antibody after cessation of protein synthesis (Figure 3A, middle panel). The 6myc-Hmg2p was more stable in the mutant than in wild type. Furthermore, comparison of the 0 h lanes demonstrated that the steady-state levels of the 6myc protein was elevated in the mutant, presumably as a result of slowed degradation. Finally, the 6myc-Hmg2p protein was also stabilized in a pulse-chase experiment, but the synthesis rates of the protein, as approximated from the pulse-labeled intensity at time 0, were comparable between the mutant and wild type (Figure 3A, right panel). The similarity in the initial amount of pulse-labeled protein between the mutant and parent strain indicated that the primary defect of the mutants was in the degradation of the 6myc-Hmg2p protein. All mutants described here showed similar mutant phenotypes: increased lovastatin resistance, elevated steady-state levels of 6myc-Hmg2p, and slowed degradation of this protein measured both by immunoblotting or by pulse-chase experiments.

### *Analysis of the hrd Mutations*

The *HRD* selection was sufficiently powerful to allow selection of mutants from a nonmutagenized culture. Eleven independent mutants were isolated that passed all of the phenotypic tests. Heterozygous diploids formed by mating each mutant to an isogenic parent strain with the opposite mating type were all sensitive to lovastatin and degraded 6myc-Hmg2p at nearly wild-type rates. Therefore, all mutants were recessive to wild type for lovastatin resistance and stabilization of 6myc-Hmg2p. Sporulation of these heterozygous diploids and analysis of phenotypes of the meiotic progeny revealed that the lovastatin resistance and stabilization of the 6myc-Hmg2p protein cosegregated. At least 20 tetrads were analyzed for each heterozygous diploid. Nine of the 11 mutations segregated as single Mendelian alleles into the meiotic progeny, giving a pattern of 2:2 Hrd$^-$:Hrd$^+$ as shown for the *hrd1-1* mutant in Figure 3B. The remaining two mutants showed a segregation pattern consistent with two unlinked mutations that were both required for the Hrd$^-$ phenotype. Although these two mutants were not studied further, their isolation indicated the power of the HRD selection, since these double mutations were selected from nonmutagenized cells.

### *Three HRD Genes*

The nine remaining mutants were characterized by complementation analysis. *hrd* mutants of each mating type were recovered from the meiotic progeny described above. These segregants were used to make heterozygous diploids between pairs of the various *hrd* mutants. The resulting diploids were then analyzed for lovastatin sensitivity and subsequently sporulated, dissected, and tested for the segregation of the mutant phenotypes into the meiotic progeny. The results of these tests indicated that the nine single recessive mutations fell into three unlinked complementation groups. The underlying wild-type genes

were referred to as *HRD1*, *HRD2*, and *HRD3*. Among the nine independent isolates, five were *hrd1* mutants, three were *hrd3* mutants, and *hrd2* was represented by a single allele.

### *Mutants Stabilized Normal Hmg2p*

The 6myc-Hmg2p protein structure was sufficiently different from the parent protein to abrogate regulation of degradation (Figure 1). Since there are examples where a mutant protein is degraded differently from its wild-type counterpart (Papavassiliou *et al.*, 1992; Tsuji *et al.*, 1992), it was important to determine whether the mutants obtained from the HRD selection were deficient in the degradation of normal Hmg2p. Accordingly, all isolated mutants were cured of the 6myc-Hmg2p-expression plasmid, retransformed with a plasmid expressing the *HMG2* gene from the same GAPDH promoter, and tested for degradation of Hmg2p. In all cases, the mutants stabilized the natural Hmg2p (Figure 4). This experiment was a cycloheximide-chase analysis of Hmg2p in wild-type (left pair) or isogenic strains with single representative mutations, *hrd1-1*, *hrd2-1*, and *hrd3-1*. Each strain had elevated steady-state levels of the Hmg2p and a concomitant stabilization of that protein. Of importance, the degree to which a given mutant affected the steady-state levels of the 6myc-Hmg2p and wild-type Hmg2p was similar. For example, the *hrd1-1* mutation caused a strong stabilization of 6myc-Hmg2p and a correspondingly high resistance to lovastatin. In contrast, the *hrd2-1* mutation stabilized the 6myc-Hmg2p protein to a lesser extent and was relatively less resistant to lovastatin. Similarly, the *hrd1-1* mutation also has a greater effect on the size and stability of the Hmg2p pool than did the *hrd2-1* mutation. In addition to the three mutants featured in Figure 4, all isolates from the *HRD* selection stabilized both Hmg2p and 6myc-Hmg2p.

The ability of *hrd* mutants to stabilize authentic Hmg2p established that the *HRD* genes encoded bona fide components of a mechanism for degrading Hmg2p. We were interested in determining whether *hrd* mutants would similarly affect the stability of the Hmg2p-GFP. This Hmg2-GFP fusion protein is degraded and regulated in a manner similar to normal Hmg2p (Hampton *et al.*, 1996). However, this fusion protein lacks the entire catalytic domain and thus offered a test of whether the membrane-associated domain of Hmg2p was sufficient to confer HRD-mediated degradation of a heterologous protein. The Hmg2-GFP reporter protein was strongly stabilized when expressed in a *hrd1-1* strain (Figure 5). A parallel analysis of the GFP reporter degradation by fluorescence-activated cell sorting analysis confirmed the results from microscopy with large numbers of cells (>10,000/strain). Furthermore, fluorescence-activated cell sorting analysis of *hrd1-1*, *hrd2-1*, and *hrd3-1* mutants corroborated the observation that the *hrd1-1* and *hrd3-1* mutants had stronger degradation phenotypes than the *hrd2-1* mutant (our unpublished observation). Thus, the membrane-associated region of Hmg2p was sufficient for HRD-mediated degradation of fusion proteins.

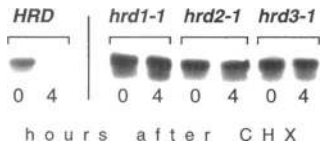


**Figure 4.** *hrd* mutants stabilized normal Hmg2p. Otherwise isogenic strains with the indicated *hrd* genotype and expressing normal Hmg2p in place of the original 6myc-Hmg2p were tested for the degradation of the Hmg2p protein by cycloheximide (CHX) chase, as in Figure 3A, middle panel. Hmg2p was detected with affinity-purified anti-Hmg1p antibody.

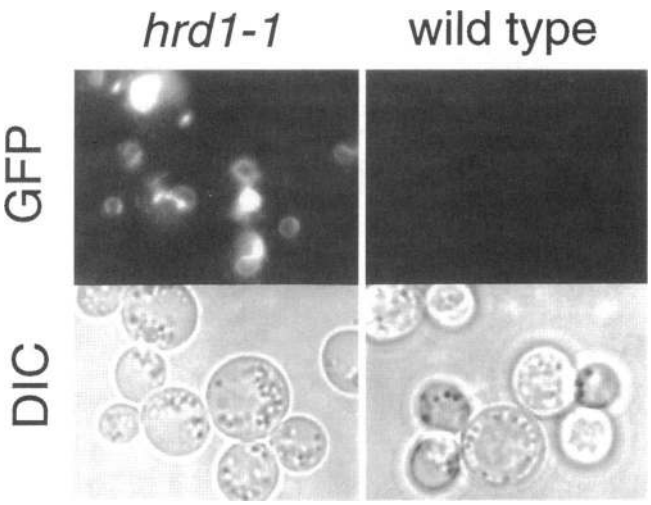


**Figure 5.** Stabilization of Hmg2p-GFP by the *hrd1-1* mutation. The degradation of Hmg2p-GFP in wild-type *HRD1* (RHY513) and mutant *hrd1-1* (RHY514) alleles. Each strain was grown into stationary phase for 12 h after entering mid-log phase and then examined directly by fluorescence microscopy for GFP fluorescence. Top panels (labeled GFP), GFP fluorescence; bottom panels (labeled DIC), Nomarski images of the same group of cells. Although the number of cells in the image is small, the same differences were observed in each of many fields examined.

The *hrd* mutants were tested for growth at various temperatures, since many classes of mutants with deficiencies in protein degradation are temperature sensitive (Finley and Chau, 1991; Hilt and Wolf, 1995). The *hrd2-1* mutant was growth-compromised, with a growth rate about 60% of the wild-type strain at all temperatures tested, but was not temperature sensitive. The growth defect of the *hrd2-1* strain cosegregated with lovastatin resistance in the haploid progeny from a cross with the isogenic parent strain, indicating that the growth defect was a consequence of the *hrd2-1* mutation. In contrast, all of the *hrd1* and *hrd3* mutants were robust and grew at rates compara-

ble to the wild-type parent strain at all temperatures tested.

### *Cloning of the HRD Genes*

Plasmids that complemented *hrd1-1*, *hrd2-1*, or *hrd3-1* were cloned by transformation of the appropriate strains with a YCp50-based genomic library and replica plating transformants onto lovastatin-containing medium. Plasmids were recovered from transformants that had regained wild-type sensitivity to lovastatin and retested for their ability to complement the appropriate mutants. In each case, the candidate plasmid also complemented the defect in 6myc-Hmg2p degradation. The identities of the yeast genomic DNA in each plasmid were determined by sequencing a small portion of each insert with a sequencing primer derived from the regions of the YCp50 parent vector that flanked the *Bam*HI insert site. These sequences were compared with sequences in national databases to determine the sequence and restriction maps of each gene. This information was then used to test all candidate coding regions by subcloning and testing for complementation. The genetic linkage of the cloned gene to the mutant loci was tested as described above.

### *HRD2 Gene Encoded a Subunit of the 26S Proteasome*

The coding region (YHR027c) that complemented the *hrd2-1* mutant encodes a 109-kDa protein that was homologous throughout (40% identical and 65% similar) to a human protein that has been proposed to be a subunit of the 26S proteasome (Figure 6). The human protein, referred to as p97, is a member of the PA700 complex that binds to and activates the mammalian 20S proteasome in vitro. Thus, the combined PA700-20S complex has been posited to be the eukaryotic 26S proteasome (DeMartino *et al.*, 1994). It would appear that the YHR027c coding region was the yeast version of the p97 subunit of the proteasomal PA700 complex. The p97 coding region was first isolated in a search for proteins that can interact with the 55-kDa tumor necrosis factor (TNF) receptor and was referred to in that work as TRAP-2 (Song *et al.*, 1995). A slightly longer version of the same coding region (908aa vs. 853aa) was subsequently deposited into GenBank (accession number D78151), as that encoding human 26S proteasome subunit p97, by the laboratory of K. Tanaka.

### *HRD2 Was a Functional TRAP-2/p97 Homologue*

The slow growth phenotype of the *hrd2-1* mutants would be consistent with Hrd2p being a proteasomal

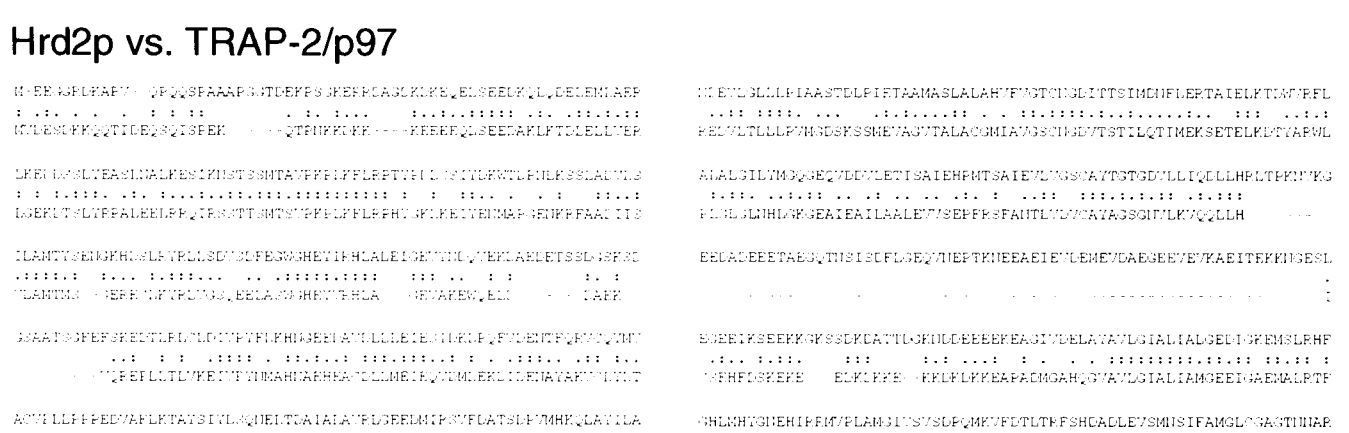


**Figure 6.** Comparison of the Hrd2p sequence and that of TRAP-2/p97, a subunit from the PA700 complex of the 26S proteasome. The *HRD2* predicted coding region (top line, YHR027c) was compared with the sequence of p97/TRAP-2 (bottom line). The program ALIGN was used, at the URL (http://vega.crbm.cnrs-mop.fr/fasta/align-query.html). The 41% identity represented by the double dots was spread throughout the sequence of the protein.

component. We further investigated this possibility by examining several other phenotypes. We tested the sensitivity of the *hrd2 -1* mutant to canavanine, an amino acid analogue of arginine which often shows heightened toxicity toward yeast strains with deficiencies in proteasomal components (Hilt and Wolf, 1995). Only *hrd2* mutants had heightened sensitivity to canavanine (Figure 7A). All alleles of *hrd1* or *hrd3* were no more sensitive to canavanine than was the isogenic parent strain. The proteasome is the site of degradation of many, but not all, ubiquitinated proteins (Egner and Kuchler, 1996; Hicke and Riezman, 1996). Therefore, mutations in proteasome components often result in a general increase in the steady-state levels of ubiquitinated proteins since the degradation rate of these intermediates is decreased when the proteasome is compromised (Papa and Hochstrasser, 1993; Hilt and Wolf, 1995). Therefore, the amount of ubiquitin immunoreactivity in whole-cell lysates, which was visualized as a characteristic ladder in whole-cell lysates, was compared in wild-type, *hrd1-1*, *hrd2-1* and *hrd3-1* strains (see below; Figure 7). Only the *hrd2-1* strain showed an elevation in the intensity of the ubiquitin immunoreactivity. Although the increase of intensity of the multiple bands was on the order of threefold, the protein transferred to the immunoblots in each lane was identical as assessed by protein staining (our unpublished observations), and all lystes were from otherwise isogenic strains. Thus the increased immunoreactivity was due to the effects of the *hrd2-1* mutation on the presence of low-level immnoreactivity (as opposed to changes in gross protein levels), with the most likely candidates being ubiquitinated degradative intermediates. Finally, expressing the human TRAP-2 coding region in the *hrd2-1* strain restored wild-type sensitivity to lovastatin (Figure 7C) and wild-type rapid degradation of 6myc-Hmg2p (our unpublished observation).

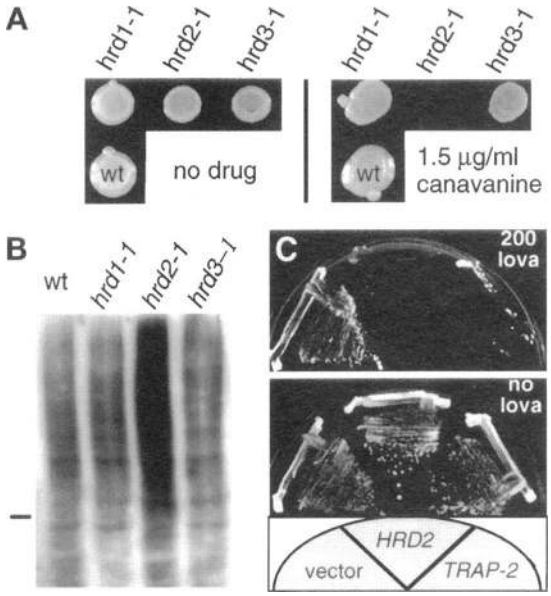


**Figure 7.** Proteasomal phenotypes associate with the *hrd2-1* mutant. (A) Canavanine sensitivity. Liquid cultures of strains with the indicated mutations, but otherwise isogenic, were spotted onto supplemented minimal medium (20 ml of ~0.5 OD) with or without 1.5 μg/ml canavanine as indicated and allowed to grow at 30°C for 1 week. (B) Global ubiquitination. Lysates of the same strains were immunoblotted with affinity-purified antiubiquitin antibody to survey the degree of ubiquitination of cellular proteins. The line indicates the position of an 80-kDa marker. Equal amounts of protein were loaded in each lane and the transfer efficiency from each lane was identical, as judged by India ink staining. The average increase in the amount of ubiquitin conjugates in the *hrd2-1* mutant was approximately threefold over the amount in other strains. (C) Complementation of the *hrd2-1* mutant by the human TRAP-2 coding region. Strain RHY402 (*hrd2-1*, Ura$^-$) was transformed with parent vector pRH98-1, with a centromere plasmid containing the *HRD2* gene (pRH482) or with a plasmid that expressed the TRAP-2 coding region from the GAPDH promoter (pRH492). These transformants are noted vector, *HRD2*, and *TRAP-2*, respectively. Each strain was then streaked on solid medium with 0 (top) or 200 μg/ml (bottom) and allowed to grow at 37°C.

Since many proteasomal proteins are essential for viability, we evaluated the phenotype of a *hrd2*Δ null by disrupting the gene in a wild-type diploid, and then sporulated the resultant heterozygous diploid to assess the viability of the haploid progeny. In all tetrads dissected, there were two live and two dead segregants, and none of the live haploids bore the marker gene (*URA3*) used to disrupt the *HRD2* gene. Thus, at least in this strain background, the *HRD2* gene was essential. Taken together, the combined phenotypes associated with the *HRD2* gene (canavanine sensitivity, slow growth of the hypomorph, lethality of the null allele, ubiquitin conjugate buildup, and complementation by human TRAP-2) all corroborated the identity of Hrd2p as the yeast homologue and analogue of the mammalian p97 subunit. Moreover, these data provided in vivo evidence that Hrd2p/TRAP2 is a functional component of the 26S proteosome.

### *Both HRD1 and HRD3 Genes Encoded Novel Proteins*

Analysis of the sequences of the *HRD1* and *HRD3* genes indicated that each encoded a novel protein (Figure 8). Both proteins appeared to have membrane-spanning domains. The *HRD3* gene encoded a protein with four features consistent with Hrd3p being a transmembrane protein oriented with the amino terminus on the lumenal site of a membrane (Sipos and von Heijne, 1993, and references therein, and Doolittle, personal communication). These features included a candidate cleavable hydrophobic N-terminal signal sequence, several asparagine-linked glycosylation consensus sites (NxT/S) in the hydrophilic region following the signal sequence, a hydrophobic region

## Hrd1p

MVPENRRKQLAIFVVVTYLLTFYCVYSATKTSVSFLQVTLKLNEGFNLMVL
SIFILLNSTLLWQLLTKLLFGELRLIEHEHIFERLPFTIINTLFMSSLFHE
RYFFTVAFFGLLLLYLKVFHWILKDRLEALLQSINDSTTMKTLIFSRFSFN
LVLLAVVDYQIITRCISSIYTNQKSDIESTSLYLIQVMEFTMLLIDLLNLF
LQTCLNFWEFYRSQQSLSNENNHIVHGDPTDENTVESDQSQPVLNDDDDDD
DDDRQFTGLEGKFMYEKAIDVFTRFLKTALHLSMLIPFRMPMMLLKDVVWD
ILALYQSGTSLWKIWRNNKQLDDTLVTVTVEQLQNSANDDNICIICMDELI
HSPNQQTWKNKNKKPKRLPCGHILHLSCLKNWMERSQTCPICRLPVFDEKG
NVVQTTFTSNSDITTQTTVTDSTGIATDQQGFANEVDLLPTRTTSPDIRIV
PTQNIDTLAMRTRSTSTPSPTWYTFPLHKTGDNSVGSSRSAYEFLITNSDE
KENGIPVKLTIENHEVNSLHGDGGEQIAKKIVIPDKFIQHI

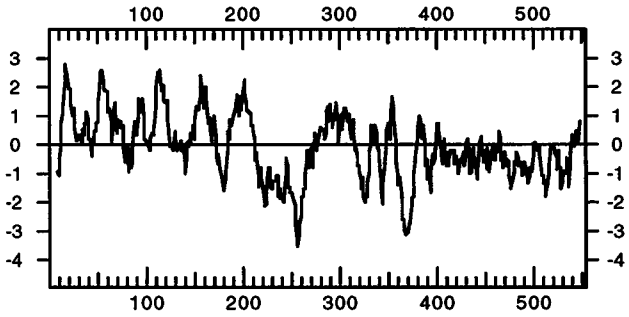


## Hrd3p

MITLLLYLCVICNAIVLIRADSIADPWPEARHLLNTIAKSRDPMKEAAMEP
NADEFVGFYVPMDYSPRNEEKNYQSIWQNEITDSQRHIYELLVQSSEQFNN
SEATYTLSQIHLWSQYNFPHNMTLAHKYLEKFNDLTHFTNHSAIFDLAVMY
ATGGCASGNDQTVIPQDSAKALLYYQRAAQLGNLKAKQVLAYKYYSGFNVP
RNFHKSLVLYRDIAEQLRKSYSRDEWDIVFPYWESYNVRISDFESGLLGKG
LNSVPSSTVRKRTTRPDIGSPFIAQVNGVQMTLQIEPMGRFAFNGNDGNIN
GDEDDEDASERRIIRIYYAALNDYKGTYSQSRNCERAKNLLELTYKEFQPH
VDNLDPLQVFYYVRCLQLLGHMYFTGEGSSKPNIHMAEEILTTSLEISRRA
QGPIGRACIDLGLINQYITNNISQAISYYMKAMKTQANNGIVEFQLSKLAT
SFPEEKIGDPFNLMETAYLNGFIPAIYEFAVMIESGMNSKSSVENTAYLFK
TFVDKNEAIMAPKLRTAFAALINDRSEVALWAYSQLAEQGYETAQVSAAYL
MYQLPYEFEDPPRTTDQRKTLAISYYTRAFKQGNIDAGVVAGDIYFQMQNY
SKAMALYQGAALKYSIQAIWNLGYMHEHGLGVNRDFHLAKRYYDQVSEHDH
RFYLASKLSVLKLHLKSWLTWITREKVNYWKPSSPLNPNEDTQHSKTSWYK
QLTKILQRMRHKEDSDKAAEDSHKHRTVVQNGANHRGDDQEEASEILGFQM
EDLVTMGCILGIFLLSILMSTLAARRGWNVRFNGAQLNANGNRQQEQQQQQ
QAQGPPGWDFNVQIFAI

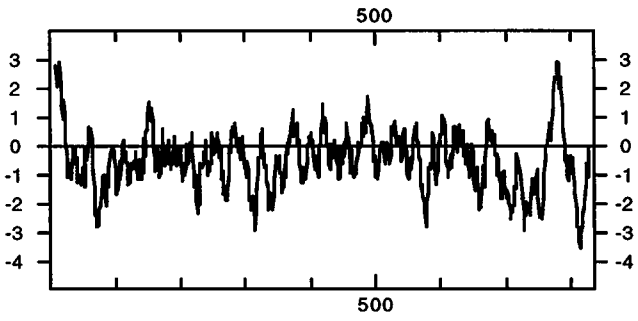


**Figure 8.** Sequences and hydropathy plots of the Hrd1p and Hrd3p predicted proteins. Strongest hydrophobic regions are underlined and in boldface. Only the first two hydrophobic regions are labeled in the Hrd1p protein (left), since these are the only ones with no charged amino acids in the 20-amino acid window. The putative signal sequence of the Hrd3p peptide is also in boldface. The plots were generated by the Kyte and Doolittle algorithm using the program DNA Strider.

of 22 amino acids with flanking charge density and hydrophobic moment predicted for a transmembrane span, and a relatively small cytoplasmic domain with a stop-transfer sequence immediately adjacent to the transmembrane span. By this model, the short C-terminal region following that transmembrane region would be in the cytosol.

The sequence of *HRD3* was used to design oligonucleotides to generate a disrupting polymerase chain reaction product that would exactly replace the predicted coding region with the *URA3* gene (Lorenz *et al.*, 1995). The disruption was successfully produced in the haploid parent strain used in the HRD selection. The resulting $Ura^+$ transformants in which the marker gene replaced the *HRD3* coding region were all strongly $Hrd^-$, i.e., they were resistant to lovastatin and displayed stabilization of the 6myc-Hmg2p reporter. These observations indicated that the *HRD3* gene was not essential, but was required for the degradation of 6myc-Hmg2p and related substrates. In spite of the strong $Hrd^-$ phenotypes, the *hrd3*Δ strain had none of the pleiotropies associated with global deficiencies in protein degradation characteristic of the *hrd2-1* mutant and other mutants with proteasomal deficiencies.

The Hrd1p protein was also novel. Again, the protein appeared to have multiple segments that could span membranes (Figure 8). The hydropathy plot of the predicted Hrd1p protein was more complex than the simple pattern of Hrd3p, and thus the number of transmembrane domains and putative orientation of the protein was harder to predict. However, it appeared that the N-terminus had more than one transmembrane span, followed by a segment with hydrophobic patches of insufficient length to span a membrane, and a hydrophilic C-terminal region. The first two hydrophobic regions, which are also the longest, are underlined in the Hrd1p sequence in Figure 8. A simple yet tentative model for Hrd1p's structure posits an amino terminal membrane-associated region with a C-terminal cytosolic domain.

The library plasmid bearing *HRD1* was used to make a disruption cassette by insertion of the functional *URA3* gene into a gap in the *HRD1* coding region created by the removal of a 750-bp *Bst*EII fragment directly centered in the coding region. Transformants of the haploid parent strain to $Ura^+$ with an *Sph*I/*Sal*I fragment resulted in lovastatin-resistant $Ura^+$ transformants. Furthermore, the lovastatin resistance was allelic to the *hrd1-1* mutation and coupled to the *URA3* marker. However, the transformation of haploids with the disruption fragment reliably resulted in ~10 times fewer colonies than identical transformation of a homozygous diploid. Dissection of the diploid resulted in four viable progeny, and the two $Ura^+$ offspring showed enhanced lovastatin reisistance. These results indicated that the *HRD1* null mutation can be generated in a haploid, but that there are perhaps other physiological consequences that must be overcome in the haploid to harbor the null phenotype. We are currently investigating these functional features of the *HRD1* gene.

## DISCUSSION

These studies represent the beginning of a systematic analysis of how HMG-R is degraded and how the degradation is regulated. Our results indicated that the degradation of HMG-R involved the 26S proteasome, possibly working in tandem with at least two novel proteins to bring about the degradation of Hmg2p. The results of our studies bring several key issues into focus and will guide related studies on the general phenomenon of membrane protein degradation and the particular mechanisms that are used by eukaryotic cells to measure and modulate the mevalonate pathway.

In previous studies, we established that degradation of Hmg2p and Hmg2-GFP fusion protein is regulated by the flux through the mevalonate pathway, so that degradation is slowed when the flux is lowered, such as by treatment of cells with lovastatin. The 6myc-Hmg2p protein, constructed in this study, was refractory to the stabilization that occurs in cells with reduced flux through this pathway. Thus, the amino acid sequence between the first and second of the transmembrane domains of Hmg2p, which are substituted by myc epitopes in the 6myc-Hmg2p, must contribute to the regulation of Hmg2p's degradation. Whether this tract of amino acids is providing specific linear determinants or structural information needed for regulation is currently being evaluated. In any event, the inability of 6myc-Hmg2p to be stablized allowed the isolation of *hrd* mutants defective in Hmg2p degradation.

Mutants in *HRD* genes, which stablized Hmg2p, also stabilized wild-type Hmg2p and an Hmg2-GFP fusion protein. Therefore, the *HRD* genes were part of a mechanism for degrading bona fide HMG-R rather than a mechanism for degrading mutant or misfolded proteins. Moreover, the stabilization of the Hmg2-GFP fusion proteins established that the membrane-associated region of Hmg2p was sufficient to confer *HRD*-mediated degradation.

The selection of Hrd mutants and the analysis of the genes identified in this screen offered a window into how HMG-R and potentially other membrane proteins are degraded.

### *HRD Genes*

The *HRD2* gene encoded the yeast homologue of a mammalian protein associated with the 26S proteasome. This mammalian protein known as TRAP-2 and as p97 protein was first purified by DeMartino *et al.* (1994) as part of the PA700 complex which associates with the core 20S proteasomal particle. The association of the PA700 complex with the 20S proteasome particle results in the formation of a 26S particle which is proposed to be the mature 26S proteasome. Hrd2p was also significantly homologous, albeit to a much lesser extent, to the yeast SEM3p protein. SEM3p has recently been shown to be a distinct component of the yeast 26S proteasome, corresponding to the p112 protein of the PA700 complex (DeMarini *et al.*, 1995). Consistent with these sequence similarities, the *hrd2-1* mutants had numerous phenotypes consistent with a deficiency in proteasomal function including slow growth, canavanine sensitivity, a global increase of ubiquitin-conjugated proteins, and complementation by the human homologue TRAP-2. Furthermore, a *hrd2::URA3* null allele caused lethality, indicating that the *HRD2* gene was essential for viability in at least some strains. The most straightforward interpretation of these data was that the proteasome plays a role in the degradation of the Hmg2p protein and related substrates such as the unregulated 6myc-Hmg2p substrate. Our data on the *hrd2-1* mutant also lend in vivo support to the hypothesis that the PA700 complex is important in the global functions of the 26S proteasome.

The identity of the Hrd2p protein as a proteasomal activator implied that the proteasome was involved in the degradation of HMG-R in yeast. These data provided a genetic counterpart to the biochemical studies implicating the proteasome in the ER degradation of the integral membrane protein CFTR and its clinically important Δ508 variant (Jensen *et al.*, 1995; Ward *et al.*, 1995). Moreover, our data indicated that the proteasome may play a broader role in the degradation of membrane proteins of the ER and possibly those of other cellular compartments also. Previous studies on mammalian cells have shown that the degradation of mammalian HMG-R is inhibited by the peptidyl-aldehyde ALLN (Inoue *et al.*, 1991; Lecureux and Watten-

berg, 1994). Originally, this inhibition was interpreted to mean that HMG-R degradation included the action of a cysteine protease. However, this agent is also a potent inhibitor of the proteasome (Jensen *et al.*, 1995). New studies with other inhibitors, as well as in vitro biochemical approaches, now indicate that inhibition of mammalian HMG-R degradation by ALLN may in fact be due to its actions on the proteasome (Simoni, personal communication).

How does a membrane protein such a Hmg2p get delivered to the proteasome for degradation? In the two simplest models, either the Hmg2p is removed from the membrane and delivered to the cytosolic proteasome or a fraction of the proteasomes associates with the ER membrane in the proximity of the Hmg2p. With regard to the possibility that the proteasome may associate with the ER membrane, it is intriguing that the human homologue of the Hrd2p proteins, known as TRAP-2, was isolated in a two-hybrid search for proteins that interact with the cytoplasmic tail of the 55-kDa TNF receptor, implying a potential association of the proteosome with a protein in the plasma membrane. Moreover, the TRAP-2 protein can be coimmunoprecipitated with the cytoplasmic domain of the 55-kDa TNF receptor (Donner, personal communication). These results suggest that the Hrd2p/TRAP-2 subunits of the proteasome could have a conserved role in anchoring the proteasome to membranes through interactions with integral membrane proteins. Because the *hrd2-1* mutants had pleiotropic phenotypes associated with proteasomal defects, the degree to which the Hrd2p/TRAP-2 protein plays a specific role in the degradation of Hmg2p, as opposed to simply being important for proteasome function, is an open question and is under active investigation.

In contrast to *HRD2*, the *HRD1* and *HRD3* genes each encode proteins that have no other known biochemical functions. Furthermore, none of the *hrd1* and *hrd3* mutants had any of the pleiotropic phenotypes associated with the *hrd2-1* mutant and with many other protein degradation mutants. However, mutants defective in *HRD1* or *HRD3* are phenotypically stronger than the *hrd2-1* mutant at stabilizing Hmg2p, in spite of the lack of other phenotypes. Presumably, the Hrd1p and Hrd3p proteins have fewer functions than the globally employed Hrd2p proteasomal subunit. Perhaps they act at an early or specific step in the delivery of the Hmg2p protein to the 26S proteasome. Alternatively, they may be involved in a separate degradation pathway for Hmg2p that is more specific for this class of substrates. The prevalence of the proteasome in degradation processes favors the former model. Since both Hrd1p and Hrd3p appear to be membrane proteins, their possible functions could include recruitment of Hmg2p to the degradation pathway, removal of Hmg2p from the ER membrane, or assembly of a degradation complex that includes a subset of 26S proteasomes bound to the ER membrane. However, our observation that the disruption of the *HRD1* gene appeared to cause transient problems in haploid survival may mean that the *HRD1* gene has broader cellular functions than the *HRD3* gene. One possibility is that Hrd1p is involved in the degradation of a larger repertoire of substrates than is Hrd3p and therefore its loss causes a larger, albeit transient, perturbation. At present, we have not examined the role of the less pleiotropic Hrd1p or Hrd3p in the degradation of other proteins, although clearly this will be a central focus in our future studies.

The C-terminal region of the predicted Hrd1p contained a member of the motif class called an H2 ring finger based on both the order and distance of the cysteine and histidine residues and the flanking amino acids (Freemont, 1993). Although the function of the H2 ring finger is not known, it has been proposed to bind $Zn^{2+}$ ions and may be involved in the interaction of the "ringed" protein with other proteins. Interestingly, this particular class of ring fingers is most common in membrane proteins, and the H2 variant of the ring finger is more likely to be found in the C-terminal region of such proteins. The role of the Hrd1p ring finger motif is under study, with a goal of identifying the other proteins that might interact with Hrd1p through this conserved region.

The most obvious feature of the Hrd3p protein is that the majority of the sequence is predicted to be in the lumen of a membrane-bound compartment, presumably the ER, and not in the cytosol, where the 26S proteasome is found. In this sense, Hrd3p is reminiscent of the US11 protein of human cytomegalovirus. US11 appears to function in the degradation of unloaded (ER localized) MHC class I molecules by causing their retrotranslocation out of the ER membrane and into the cytosol for degradation by the proteasome (Wiertz *et al.*, 1996). Since the degradation of HMG-R appears to be a processive process, a similar function may be required for the presentation of polytopic substrates such as HMG-R to the cytosolic 26S proteasome. Parallel studies on the degradation of soluble proteins of the ER lumen have hinted that the proteasome may also be involved in the degradation of those proteins as well, and some evidence supporting retrotranslocation to the cytosol has been provided for this class of substrates (McCracken and Brodsky, 1996). Thus, it may be that the movement of peptide sequences, either as part of polytopic membrane proteins or as free lumenal proteins, from protected lumenal regions to the cytosolic proteasome is a common theme in the ER degradation of a disparate set of proteins.

### *Hrd3p Homologues and the HRD3 Motif*

The Hrd1p and Hrd3p proteins are not full-length homologues of well-studied proteins, as is Hrd2p. However, the Hrd3p protein contains a region homologous to numerous proteins. The most homologous portion of *HRD3* is in the region of aa 625–666. This sequence has significant homology to regions of human, *C. elegans*, and *S. pombe* proteins in the public databases (Figure 9). Furthermore, this region of Hrd3p also has homology to a more N-terminal portion of the Hrd3p protein itself, implying that the evolution of the modern sequence might have included an ancient duplication of the conserved motif. The *C. elegans* protein sel-1 is the highest scoring Hrd3p orthologue in the database. The overall identity of sel-1 and Hrd3p is ~20%, with regions that are much higher (Figure 9). The predicted sel-1 protein also appears to have a similarly duplicated region as well as regions of homology to Hrd3p outside of the duplicated motif. Unlike the Hrd3p peptide, the sel-1 protein has no C-terminal transmembrane region, but rather resembles a version of the Hrd3p protein that is terminated before the transmembrane span. The first 80 amino acids of the sel-1 protein encodes a functional signal sequence. Based on these features, the sel-1 protein was predicted to be extracellular (Grant and Greenwald, 1996). However, sel-1 may be associated with intracellular vesicles (Grant and Greenwald, personal communication).

There is also a homologue of Hrd3p in yeast itself called Skt5p. Although significanly less similar to the Hrd3p protein than sel-1, the characteristic Hrd3p motif is present, and an ancient duplication of the motif is present in a more N-terminal part of the protein, as in sel-1 and Hrd3p. Furthermore, it appears that the Skt5p C-terminus has a farnesylation site. Thus, the Hrd3p and Skt5p protiens appear to have distinct, familiar features that allow membrane association: a transmembrane span or a farnesylation site, respectively. Perhaps the conserved function(s) of the Hrd3 motif somehow requires proximity of the C-terminus to a membrane, as promoted by each of these distinct C-termini. In this regard, it will be interesting to learn more about the cellular location of the sel-1 protein.

Although none of the proteins with homologies to Hrd3p have a well-understood function, *sel-1* mutants have some suggestive phenotypes. *sel-1* was isolated as a suppresser of a hypomorphic mutation in the *lin-12*-encoded transmembrane receptor. The same *sel-1* mutation also partly relieves the phenotype of a hypomorphic mutation in the related but distinct *glp-1*-encoded transmembrane receptor. The original *sel-1* mutation appears to be a null allele. Accordingly, the sel-1 protein is described as a negative regulator of each of these receptors since less *sel-1* activity results in more lin-2 and more glp-1 signals from the mutant proteins. Of importance, the *sel-1* mutation cannot bypass null mutations of either *lin-12* or *glp-1*. Furthermore, the *sel-1* mutation has no phenotype in worms with wild-type *lin-12* and *glp-1* genes. It may be that the sel-1 protein is involved in the degradation of hypomorphic lin-12 and glp-1 proteins. In this way, the loss of *sel-1* function might suppress the mutant phenotypes by allowing elevated levels of the degraded mutant receptors much as *hrd3* mutants increase the level of Hmg2p. However, it is certainly possible that the homology is due to shared motifs that function in very distinct ways.

### *HRD Genes and the Mevalonate Pathway*

The HRD selection presented in this work relied on the use of a variant of Hmg2p whose half-life was not affected by alterations of the mevalonate pathway. Nevertheless, the resulting mutants all stabilized normal Hmg2p. Thus, the *HRD* gene-encoded degradation process cannot distinguish between regulated and unregulated degradation substrates. In contrast, alteration of the mevalonate pathway only affects the degradation of normal Hmg2p and some variations of Hmg2p, such as Hmg2p-GFP but not 6myc-Hmg2p (Hampton *et al.*, 1996). Clearly, the regulation of Hmg2p degradation by the mevalonate pathway cannot occur by simply altering the action of one or more Hrd proteins. If this were the mechanism, then any protein degraded by the actions of the Hrd proteins would be regulated by the mevalonate pathway. In fact, only a subset are regulated, e.g., Hmg2p and Hmg2p-GFP. Therefore, these data indicated that the regulation of Hmg2p degradation by the mevalonate pathway occurs by altering the susceptibility of a regulated protein to degradation by the *HRD*-encoded machinery.

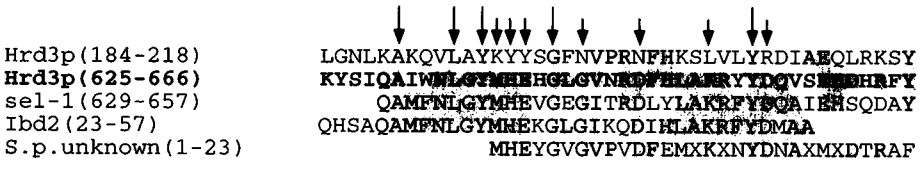


**Figure 9.** A conserved motif in Hrd3p. Alignment of a conserved region of Hrd3p with peptides from Hrd3p itself (top row), the sel-1 protein, the human Ibd2 peptide, and an *S. pombe* peptide (1236254). Long arrows indicate those amino acids that were absolutely conserved, and short arrows indicate those that were conserved between the heterologous proteins and the distal region in Hrd3p (row 2).

The HRD selection presents an opportunity to identify potentially all genes that are required for the degradation of Hmg2p and possibly other membrane proteins. Our current task is to ascertain the functional relationships of the different genes, to integrate the new genes with familiar themes and mechanisms of protein degradation, and to understand the mechanism by which the mevalonate pathway can selectively alter the susceptibility of a select group of proteins to the HRD degradation pathway.

## ACKNOWLEDGMENTS

We thank Mark Hochstrasser, Robert Simoni, and members of our laboratories for many helpful discussions and insights, as well as Barth Grant and Iva Greenwald for sharing information about the sel-1 protein prior to publication. We thank Russell Doolittle for generously providing analysis and expertise on protein sequences. We also thank Paul Herman for the YCp50-based library, Randy Schekman for 9E10 anti-myc ascites fluid, David Donner for the TRAP-2 coding region and personal communication about the TRAP-2 cDNA and protein, Arthur Haas for anti-ubiquitin antibodies, and Randy Johnson (the "Anti-Randy") for consultations on protein and PI stability. Finally, we thank Nathan Bays, Antonin Tutter, Tamara Darsow, and Sheetal Patel (all at University of California, San Diego) for diligent and cheerful participation in the HRD project. This work was supported by a Helen Hay Whitney postdoctoral fellowship, a California Chapter of the American Heart Association senior postdoctoral fellowship (R.Y.H.), generous start-up funds from the Biology Department, University of California, San Diego (R.Y.H.), and by a grant from the National Institutes of Health (GM-35827, J.R.). Core support was provided by a National Institute of Environmental Health Sciences Mutagenesis Center grant (P30ESO1896-12).

## REFERENCES

Basson, M.E., Thorsness, M., Finer, M.J., Stroud, R.M., and Rine, J. (1988). Structural and functional conservation between yeast and human 3-hydroxy-3-methylglutaryl coenzyme A reductases, the rate-limiting enzyme of sterol biosynthesis. Mol. Cell Biol. *8*, 3797–3808.

Berkower, C., Loayza, D., and Michaelis, S. (1994). Metabolic instability and constitutive endocytosis of STE6, the a-factor transporter of *Saccharomyces cerevisiae*. Mol. Biol. Cell *5*, 1185–1198.

Bienkowski, R.S. (1983). Intracellular degradation of newly synthesized secretory proteins. Biochem. J. *214*, 1–10.

Bitter, G.A., and Egan, K.M. (1984). Expression of heterologous genes in *Saccharomyces cerevisiae* from vectors utilizing the glyceraldehyde-3-phosphate dehydrogenase gene promoter. Gene *32*, 263–274.

Boeke, J.D., Trueheart, J., Natsoulis, G., and Fink, G.R. (1987). 5-fluoroorotic acid as a selective agent in yeast molecular genetics. Methods Enzymol. *154*, 164–175.

Bour, S., Schubert, U., and Strebel, K. (1995). The human immunodeficiency virus type 1 Vpu protein specifically binds to the cytoplasmic domain of CD4: implications for the mechanism of degradation. J. Virol. *69*, 1510–1520.

Chiang, H.L., and Schekman, R. (1991). Regulated import and degradation of a cytosolic protein in the yeast vacuole (see comments). Nature *350*, 313–318.

DeMarini, D.J., Papa, F.R., Swaminathan, S., Ursic, D., Rasmussen, T.P., Culbertson, M.R., and Hochstrasser, M. (1995). The yeast SEN3 gene encodes a regulatory subunit of the 26S proteasome complex required for ubiquitin-dependent protein degradation in vivo. Mol. Cell Biol. *15*, 6311–6321.

DeMartino, G.N., Moomaw, C.R., Zagnitko, O.P., Proske, R.J., Chu, P.M., Afendis, S.J., Swaffield, J.C., and Slaughter, C.A. (1994). PA700, an ATP-dependent activator of the 20 S proteasome, is an ATPase containing multiple members of a nucleotide-binding protein family. J. Biol. Chem. *269*, 20878–20884.

Dice, J.F., and Chiang, H.L. (1989). Peptide signals for protein degradation within lysosomes. Biochem. Soc. Symp. *55*, 45–55.

Edwards, P.A., Lan, S.F., Tanaka, R.D., and Fogelman, A.M. (1983). Mevalonolactone inhibits the rate of synthesis and enhances the rate of degradation of 3-hydroxy-3-methylglutaryl coenzyme A reductase in rat hepatocytes. J. Biol. Chem. *258*, 7272–7275.

Egner, R., and Kuchler, K. (1996). The yeast multidrug transporter Pdr5 of the plasma membrane is ubiquitinated prior to endocytosis and degradation in the vacuole. FEBS Lett. *378*, 177–181.

Eriksson, P., Andre, L., Ansell, R., Blomberg, A., and Adler, L. (1995). Cloning and characterization of GPD2, a second gene encoding sn-glycerol 3-phosphate dehydrogenase ($NAD^+$) in *Saccharomyces cerevisiae*, and its comparison with GPD1. Mol. Microbiol. *17*, 95–107.

Evan, G.I., Lewis, G.K., Ramsay, G., and Bishop, J.M. (1985). Isolation of monoclonal antibodies specific for human c-myc proto-oncogene product. Mol. Cell Biol. *5*, 3610–3616.

Finley, D., and Chau, V. (1991). Ubiquitination. Annu. Rev. Cell Biol. *7*, 25–69.

Freemont, P.S. (1993). The RING finger. A novel protein sequence motif related to the zinc finger. Ann. NY Acad. Sci. *684*, 174–192.

Gietz, R.D., and Sugino, A. (1988). New yeast-*Escherichia coli* shuttle vectors constructed with in vitro mutagenized yeast genes lacking six-base pair restriction sites. Gene *74*, 527–534.

Glotzer, M., Murray, A.W., and Kirschner, M.W. (1991). Cyclin is degraded by the ubiquitin pathway. Nature *349*, 132–138.

Goldstein, J.L., and Brown, M.S. (1990). Regulation of the mevalonate pathway. Nature *343*, 425–430.

Grant, B., and Greenwald, I. (1996). The *Caenorhabditis elegans sel-1* gene, a negative regulator of *lin-12* and *glp-1*, encodes a predicted extracellular protein. Genetics *143*, 237–247.

Grant, E.P., Michalek, M.T., Goldberg, A.L., and Rock, K.L. (1995). Rate of antigen degradation by the ubiquitin-proteasome pathway influences MHC class I presentation. J. Immunol. *155*, 3750–3758.

Hampton, R.Y., and Rine, J. (1994). Regulated degradation of HMG-CoA reductase, an integral membrane protein of the endoplasmic reticulum, in yeast. J. Cell Biol. *125*, 299–312.

Hampton, R.Y., Konong, A., Wright, R., and Rine, J. (1996). In vivo examination of membrane protein localization and degradation with GFP. Proc. Natl. Acad. Sci. USA *93*, 828–833.

Hicke, L., and Riezman, H. (1996). Ubiquitination of a yeast plasma membrane receptor signals its ligand-stimulated endocytosis. Cell *84*, 277–287.

Hilt, W., and Wolf, D.H. (1995). Proteasomes of the yeast *S. cerevisiae*: genes, structure and functions. Mol. Biol. Rep. *21*, 3–10.

Hochstrasser, M. (1992). Ubiquitin and intracellular protein degradation. Curr. Opin. Cell Biol. *4*, 1024–1031.

Hochstrasser, M. (1995). Ubiquitin, proteasomes, and the regulation of intracellular protein degradation. Curr. Opin. Cell Biol. *7*, 215–223.

Inoue, S., Bar, N.S., Roitelman, J., and Simoni, R.D. (1991). Inhibition of degradation of 3-hydroxy-3-methylglutaryl-coenzyme A reduc-

tase in vivo by cysteine protease inhibitors. J. Biol. Chem. *266*, 13311–13317.

Jabben, M., Shanklin, J., and Vierstra, R.D. (1989). Ubiquitin-phytochrome conjugates. Pool dynamics during in vivo phytochrome degradation. J. Biol. Chem. *264*, 4998–5005.

Jensen, T.J., Loo, M.A., Pind, S., Williams, D.B., Goldberg, A.L., and Riordan, J.R. (1995). Multiple proteolytic systems, including the proteasome, contribute to CFTR processing. Cell *83*, 129–135.

Kornitzer, D., Raboy, B., Kulka, R.G., and Fink, G.R. (1994). Regulated degradation of the transcription factor Gcn4. EMBO J. *13*, 6021–6030.

Lecureux, L.W., and Wattenberg, B.W. (1994). The regulated degradation of a 3-hydroxy-3-methylglutaryl-coenzyme A reductase reporter construct occurs in the endoplasmic reticulum. J. Cell Sci. *107*, 2635–2642.

Lorenz, M.C., Muir, R.S., Lim, E., McElver, J., Weber, S.C., and Heitman, J. (1995). Gene disruption with PCR products in *Saccharomyces cerevisiae*. Gene *158*, 113–117.

McCracken, A.A., and Brodsky, J.L. (1996). Assembly of ER-associated protein degradation in vitro: dependence on cytosol, calnexin and ATP. J. Cell Biol. *132*, 291–298.

Mullins, C., Lu, Y., Campbell, A., Fang, H., and Green, N. (1995). A mutation affecting signal peptidase inhibits degradation of an abnormal membrane protein in *Saccharomyces cerevisiae*. J. Biol. Chem. *270*, 17139–17147.

Murakami, Y., Matsufuji, S., Kameji, T., Hayashi, S., Igarashi, K., Tamura, T., Tanaka, K., and Ichihara, A. (1992). Ornithine decarboxylase is degraded by the 26S proteasome without ubiquitination. Nature *360*, 597–599.

Oda, M.N., Scott, S.V., Hefner, G.A., Caffarelli, A.D., and Klionsky, D.J. (1996). Identification of a cytoplasm to vacuole targeting determinant in aminopeptidase I. J. Cell Biol. *132*, 999-1010.

Papa, F.R., and Hochstrasser, M. (1993). The yeast DOA4 gene encodes a deubiquitinating enzyme related to a product of the human tre-2 oncogene. Nature *366*, 313–319.

Papavassiliou, A.G., Treier, M., Chavrier, C., and Bohmann, D. (1992). Targeted degradation of c-Fos, but not v-Fos, by a phosphorylation-dependent signal on c-Jun. Science *258*, 1941–1944.

Pearce, D.A., and Sherman, F. (1995). Degradation of cytochrome oxidase subunits in mutants of yeast lacking cytochrome c and suppression of the degradation by mutation of *YME1*. J. Biol. Chem. *270*, 20879–20882.

Roitelman, J., and Simoni, R.D. (1992). Distinct sterol and nonsterol signals for the regulated degradation of 3-hydroxy-3-methylglutaryl-CoA reductase. J. Biol. Chem. *267*, 25264–25273.

Rose, M.D., Novick, P., Thomas, J.H., Botstein, D., and Fink, G.R. (1987). A *Saccharomyces cerevisiae* genomic plasmid bank based on a centromere-containing shuttle vector. Gene *60*, 237–243.

Scheffner, M., Huibregtse, J.M., Vierstra, R.D., and Howley, P.M. (1993). The HPV-16 E6 and E6-AP complex functions as a ubiquitin-protein ligase in the ubiquitination of p53. Cell *75*, 495–505.

Schena, M., Picard, D., and Yamamoto, K.R. (1991). Vectors for constitutive and inducible gene expression in yeast. Methods Enzymol. *194*, 389–398.

Schork, S.M., Thumm, M., and Wolf, D.H. (1995). Catabolite inactivation of fructose-1,6-bisphosphatase of *Saccharomyces cerevisiae*. Degradation occurs via the ubiquitin pathway. J. Biol. Chem. *270*, 26446–26450.

Schuller, H.J., Fortsch, B., Rautenstrauss, B., Wolf, D.H., and Schweizer, E. (1992). Differential proteolytic sensitivity of yeast fatty acid synthetase subunits alpha and beta contributing to a balanced ratio of both fatty acid synthetase components. Eur. J. Biochem. *203*, 607–614.

Scott, S.V., and Klionsky, D.J. (1995). In vitro reconstitution of cytoplasm to vacuole protein targeting in yeast. J. Cell Biol. *131*, 1727–1735.

Sipos, L., and von Heijne, G. (1993). Predicting the topology of eukaryotic membrane proteins. Eur. J. Biochem. *213*, 1333–1340.

Song, H.Y., Dunbar, J.D., Zhang, Y.X., Guo, D., and Donner, D.B. (1995). Identification of a protein with homology to hsp90 that binds the type 1 tumor necrosis factor receptor. J. Biol. Chem. *270*, 3574–3581.

Tierney, D.J., Haas, A.L., and Koop, D.R. (1992). Degradation of cytochrome P450 2E1: selective loss after labilization of the enzyme. Arch. Biochem. Biophys. *293*, 9–16.

Tsuji, E., Misumi, Y., Fujiwara, T., Takami, N., Ogata, S., and Ikehara, Y. (1992). An active-site mutation (Gly633→Arg) of dipeptidyl peptidase IV causes its retention and rapid degradation in the endoplasmic reticulum. Biochemistry *31*, 11921–11927.

Ward, C.L., Omura, S., and Kopito, R.R. (1995). Degradation of CFTR by the ubiquitin-proteasome pathway. Cell *83*, 121–127.

Wiertz, E.J.H.J., Jones, T.R., Sun, L., Bogyo, M., Geuze, H.J., and Ploegh, H.L. (1996). The human cytomegalovirus US11 gene product dislocates MHC class I heavy chains from the endoplasmic reticulum to the cytosol. Cell *84*, 769–779.

Wilcox, C.A., Redding, K., Wright, R., and Fuller, R.S. (1992). Mutation of a tyrosine localization signal in the cytosolic tail of yeast Kex2 protease disrupts Golgi retention and results in default transport to the vacuole. Mol. Biol. Cell *3*, 1353–1371.